COMPEL—The International Journal for Computation and Mathematics in Electrical and Electronic Engineering
Vol. 4, No. 3, 123–135

METHOD OF CONFORMAL TRANSFORMATION FOR THE FINITE-ELEMENT SOLUTION OF AXISYMMETRIC EXTERIOR-FIELD PROBLEMS

S.H. WONG and I.R. CIRIC

Department of Electrical Engineering, University of Manitoba, Winnipeg, Canada, R3T 2N2

ABSTRACT: The finite-element method can be used for an approximate solution of axisymmetric exterior-field problems by truncating the unbounded domain, or by applying various techniques of coupling a finite region of interest with the remaining far region, which is properly modelled.

In this paper, we propose the solution of axisymmetric exterior-field problems by using the standard finite-element method in a bounded, transformed domain obtained by conformal mapping from the original, unbounded one. The transformed functionals have very simple expressions and the exact transforms of the original boundary conditions are used in the transformed domain. Consequently no approximation is introduced in the proposed method and improvements in the accuracy of the solution are obtained as compared with several other methods in common usage, especially with the truncated mesh technique.

A few example problems are solved and the presented method is found to be simple and computationally highly efficient. It is particularly recommended for problems with material inhomogeneities and anisotropies within large regions.

1. INTRODUCTION

The simplest procedure for implementing the finite-element method (FEM) for the solution of unbounded region field problems consists in truncating the infinite domains at a sufficiently large distance and imposing approximate conditions on the terminating boundaries. This technique, however, requires a large amount of computation to achieve acceptable accuracy.

Several techniques for improving the accuracy of the solution and the computation efficiency have been proposed based on boundary integral equation methods or on hybrid methods of coupling finite elements with integral equations [1–3].

Recently, methods of mapping have been elaborated for unbounded region field problems. A widely investigated procedure, which has become a standard practice, consists of using various local mappings defined for infinite elements [4–8], which are designed to approximate the actual field decay towards infinity. An alternative approach is to map the entire unbounded region of the problem onto a bounded transformed domain in which a numerical method, such as the FEM, is implemented. Since the two-dimensional Laplace's equation remains unchanged under conformal mapping, such an approach has been found to be computationally efficient for parallel-plane scalar fields [9].

In this paper, we present the solution of three-dimensional axisymmetric field problems by implementing the FEM in the bounded transformed domain obtained from the original one by conformal mapping. Due to the fact that the modelling and discretization of any bounded region can be performed accurately by finite elements, it is not necessary to search for problem-dependent analytic function transformations for the purpose of getting simply shaped transformed domains. Therefore, only a few standard conformal transformations, such as inversion for instance, will be sufficient for implementing the proposed method.

A major advantage of using analytic function transformations for axisymmetric field problems involving the Laplacian operator is that the form of the transformed energy functionals is very similar to that of the original ones. Consequently, this method can be implemented with any standard finite-element computer program.

The proposed method can be used for the analysis of both bounded and unbounded region axisymmetric fields, but is best suited to the solution of unbounded region field problems. A few examples are given and the solution is much better than that corresponding to the truncated mesh technique in the original domain. Even with a small number of elements, highly accurate results are obtained.

2. THEORETICAL FORMULATION

Consider a three dimensional axisymmetric scalar field described in circular cylindrical coordinates (ρ, ϕ, z), with the z-axis chosen as the axis of symmetry, by the equation

$$\frac{1}{\rho}\left\{\frac{\partial}{\partial z}\left[\rho\left(\kappa_{11}\frac{\partial \Phi}{\partial z}+\kappa_{12}\frac{\partial \Phi}{\partial \rho}\right)\right]+\frac{\partial}{\partial \rho}\left[\rho\left(\kappa_{21}\frac{\partial \Phi}{\partial z}+\kappa_{22}\frac{\partial \Phi}{\partial \rho}\right)\right]\right\}=g \tag{1}$$

In terms of the operator $\nabla \equiv \boldsymbol{a}_z(\partial/\partial z)+\boldsymbol{a}_\rho(\partial/\partial\rho)$, eq. (1) has the following concise form

$$\frac{1}{\rho}[\nabla\cdot(\rho\boldsymbol{\kappa}\cdot\nabla\Phi)]=g \tag{2}$$

The tensor $\boldsymbol{\kappa}$ describes the axisymmetric material inhomogeneities and anisotropies, and is represented by the matrix

$$\boldsymbol{\kappa}=\begin{bmatrix}\boldsymbol{\kappa}_{11}(z,\rho) & \boldsymbol{\kappa}_{12}(z,\rho)\\ \boldsymbol{\kappa}_{21}(z,\rho) & \boldsymbol{\kappa}_{22}(z,\rho)\end{bmatrix} \tag{3}$$

which is positive definite at all the points (z, ρ) for most physical media. The function $g(z, \rho)$ in eq. (2) defines the source space distribution.

Consider the domain D of the azimuthal semi-plane (Fig. 1) with the boundary C, which usually includes sections of the z-axis. The general from of the boundary conditions is of a mixed type and can be written as

$$\Phi|_{C_1}=\Phi_0(s)\,,\qquad s\in C_1 \tag{4}$$

$$[(\rho\boldsymbol{\kappa}\cdot\nabla\Phi)\cdot\boldsymbol{n}]+\sigma(s)\Phi(s)=h(s)\,,\qquad \text{on } C_2 \tag{5}$$

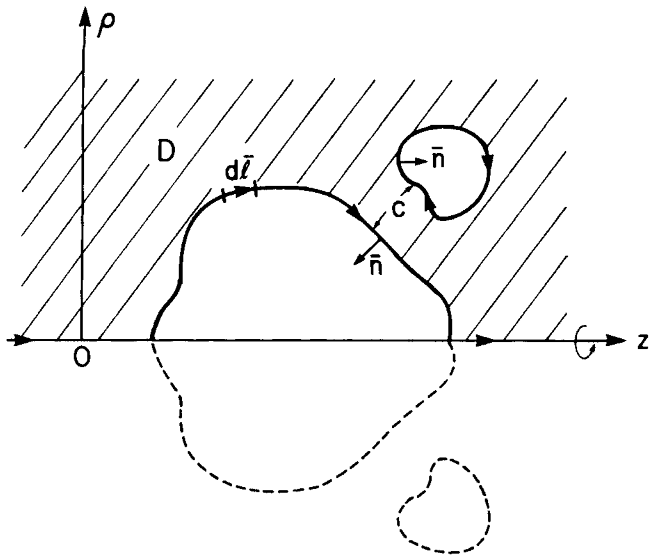

Figure 1: Azimuthal section of axisymmetric region

where $\sigma(s) \geqslant 0$, and $\boldsymbol{n}$ denotes the outward unit normal to the boundary, $C = C_1 + C_2$.

The solution of the above problem can be obtained [10] by minimizing the functional

$$F = \frac{1}{2} \int_D [(\nabla \Phi) \cdot (\rho \boldsymbol{\kappa} \cdot \nabla \Phi) + 2\rho \Phi g] \, \mathrm{d}z \, \mathrm{d}\rho + \frac{1}{2} \int_{C_2} (\sigma \Phi^2 - 2h\Phi) \, \mathrm{d}l \tag{6}$$

with trial functions which satisfy the Dirichlet condition (4). The Euler–Lagrange equation associated to the functional (6) is eq. (2), and eq. (5) is satisfied as a natural boundary condition.

Consider now the conformal mapping of the bounded domain $D' + C_1' + C_2'$ of the uv-plane onto the domain $D + C_1 + C_2$ of the $z\rho$-plane, given by the following analytic function transformation

$$z + i\rho \equiv z(u, v) + i\rho(u, v) = f(w) \tag{7}$$

where $w \equiv u + iv$ and $i \equiv \sqrt{-1}$. By using the Cauchy–Riemann conditions

$$\frac{\partial u}{\partial z} = \frac{\partial v}{\partial \rho}, \qquad \frac{\partial u}{\partial \rho} = -\frac{\partial v}{\partial z} \tag{8}$$

eq. (6) can be written in the form

$$F = \frac{1}{2} \int_{D'} \left[(\nabla' \Phi') \cdot (\rho' \boldsymbol{\kappa}' \cdot \nabla' \Phi') + 2\rho' \Phi' g' \left| \frac{\mathrm{d}f}{\mathrm{d}w} \right|^2 \right] \mathrm{d}u \, \mathrm{d}v$$

$$+ \frac{1}{2} \int_{C_2'} (\sigma' \Phi'^2 - 2h' \Phi') \left| \frac{\mathrm{d}f}{\mathrm{d}w} \right| \, \mathrm{d}l' \tag{9}$$

with $\nabla' \equiv \boldsymbol{a}_u(\partial/\partial u) + \boldsymbol{a}_v(\partial/\partial v)$ and Φ', ρ', g', σ' and h' denoting, respectively, the functions Φ, ρ, g, σ and h written explicitly in terms of u and v by means of the transformation in eq. (7). In matrix form, the tensor $\boldsymbol{\kappa}'$ is related to $\boldsymbol{\kappa}$ by

$$\boldsymbol{\kappa}' = T\boldsymbol{\kappa}T^{-1} \tag{10}$$

where the matrix T is defined as

$$T = \begin{bmatrix} \dfrac{\partial u}{\partial z} & \dfrac{\partial u}{\partial \rho} \\ \\ \dfrac{\partial v}{\partial z} & \dfrac{\partial v}{\partial \rho} \end{bmatrix} \tag{11}$$

and T^{-1} denotes its inverse.

For the two-dimensional (parallel-plane) field in the transformed domain, $\rho'\boldsymbol{\kappa}'$ can be interpreted as representing the fictitious material properties, $\rho' g' |\mathrm{d}f/\mathrm{d}w|^2$ as the corresponding source space distribution, with σ and h replaced by $\sigma'|\mathrm{d}f/\mathrm{d}w|$ and $h'|\mathrm{d}f/\mathrm{d}w|$, respectively. One can see from eq. (10) that for an isotropic but inhomogeneous medium, for which $\boldsymbol{\kappa}$ is a scalar function of position, $\boldsymbol{\kappa}'$ is also a scalar function of position. In the case of an isotropic and homogeneous medium, $\boldsymbol{\kappa}$ and $\boldsymbol{\kappa}'$ will both be the same scalar constant.

In the proposed method, the new functional in eq. (9) is to be minimized by implementing the finite-element technique in the transformed domain. The Dirichlet boundary condition in eq. (4) remains unchanged at the corresponding points on C_1' and must be enforced for all the trial functions. The given mixed boundary conditions have been directly incorporated into the new eq. (9) and as a consequence, all the boundary conditions in the bounded transformed domain are the exact transforms of the original ones. Once the transformed domain solution is obtained, the original field problem solution is recovered through mapping.

Due to the similarity in the form of the two expressions in eqs. (6) and (9), an existing standard finite-element computer program for the original domain can be used in the transformed domain. The implementation of the presented procedure does not require a new special computer program.

It should be noted that other numerical techniques may also be applied in conjunction with global mapping. If, instead of FEM, the finite-difference method is used, for instance, the transform of the governing equations must also be known. By applying the transformation in eq. (7), eqs. (2), (4) and (5) become, respectively,

$$\frac{1}{\rho'}[\nabla' \cdot (\rho'\boldsymbol{\kappa}' \cdot \nabla'\Phi')] = g'\left|\frac{\mathrm{d}f}{\mathrm{d}w}\right|^2 \quad \text{in } D' \tag{12}$$

$$\Phi|_{C_1'} = \Phi_0(s')\,, \quad s' \in C_1' \tag{13}$$

and

$$(\rho'\boldsymbol{\kappa}' \cdot \nabla'\Phi') \cdot \boldsymbol{n}' + \sigma'\Phi'\left|\frac{\mathrm{d}f}{\mathrm{d}w}\right| = h'\left|\frac{\mathrm{d}f}{\mathrm{d}w}\right| \quad \text{on } C_2' \tag{14}$$

where $\boldsymbol{n}'$ denotes the outward unit normal to C_2'. In order to implement easily a method such as the finite-difference method, it is essential for the transformed domain to be geometrically "simple", and that necessarily requires problem-dependent transformations which are not always available. This is not the case when implementing the FEM. Indeed, taking into account that any bounded region can be discretized accurately by finite elements, the geometric shape of the transformed domain is not an important factor. For the application of the proposed method, a few standard analytic function transformations will be sufficient for most practical system geometries.

3. TEST PROBLEMS

Four examples are presented in this section to test the proposed method for field problems in homogeneous media, in inhomogeneous media, as well as with external source distribution, by using two types of transformation function. In all the examples, quadratic triangular elements have been used in the finite-element analysis.

3.1. Conducting sphere in the presence of an infinite ground plane

The center of a conducting sphere of radius a is at a distance b from an equipotential infinite plane, as shown in Fig. 2. An electric potential of Φ_0 is applied to the sphere relative to the plane. The infinitely extended dielectric medium between the sphere and the plane is uncharged and is homogeneous with a permittivity ε_0. The electric potential Φ satisfies eq. (1) where $\kappa_{12} = \kappa_{21} = g = 0$ and $\kappa_{11} = \kappa_{22} = \varepsilon_0$, with the following boundary conditions

$$\Phi = \begin{cases} \Phi_0 & \text{for } (z-b)^2 + \rho^2 = a^2 \\ 0 & \text{at } z = 0 \\ 0 & \text{at infinity} \end{cases} \tag{15}$$

$$\frac{\partial \Phi}{\partial \rho} = 0 \quad \text{at } \rho = 0 \tag{16}$$

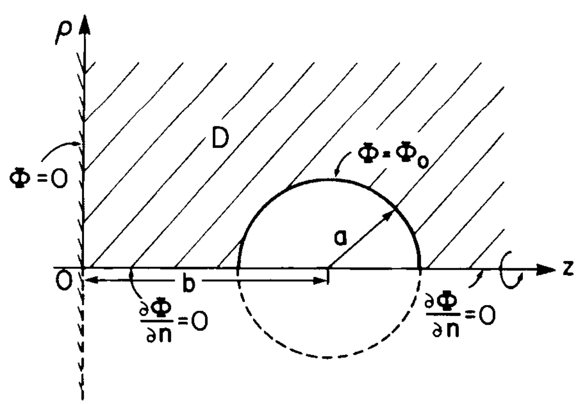

Figure 2: Azimuthal section for sphere-to-plane configuration

Using the analytic function $f(w) = c\tanh(w/2)$, where $c = a\sinh u_0$ and $u_0 = \cosh^{-1}(b/a)$, yields

$$z = \frac{c\sinh u}{\cosh u + \cos v} \tag{17}$$

$$\rho = \frac{c\sin v}{\cosh u + \cos v} \tag{18}$$

This transformation maps conformally the domain D onto the rectangular domain D' shown in Fig. 3.

The transformed functional in eq. (9) is now

$$F = \frac{\varepsilon_0}{2}\int_{D'}\left(\frac{c\sin v}{\cosh u + \cos v}\right)(\nabla'\Phi')^2\,du\,dv \tag{19}$$

and the constraints for Φ' are

$$\Phi' = \begin{cases}\Phi_0, & u = u_0\\ 0, & u = 0\end{cases} \tag{20}$$

The normalized electrostatic capacitance C of this system can be calculated from the minimum value $F_{\min}$ of the functional (19) [11] as

$$C = \frac{F_{\min}}{\varepsilon_0 a \Phi_0^2} \tag{21}$$

The problem was solved for various ratios of b/a by using the mesh presented in Fig. 3. The percentage error in the electrostatic capacitance obtained is given in Fig. 4.

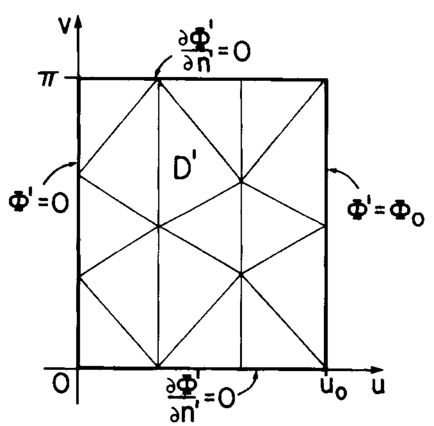

Figure 3: Finite element mesh in the transformed domain for sphere-to-plane problem

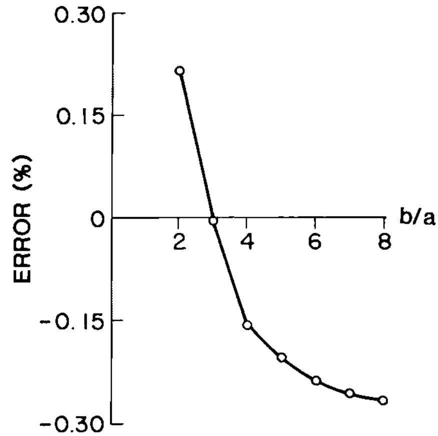

Figure 4: Error in electrostatic capacitance for sphere-to-plane system

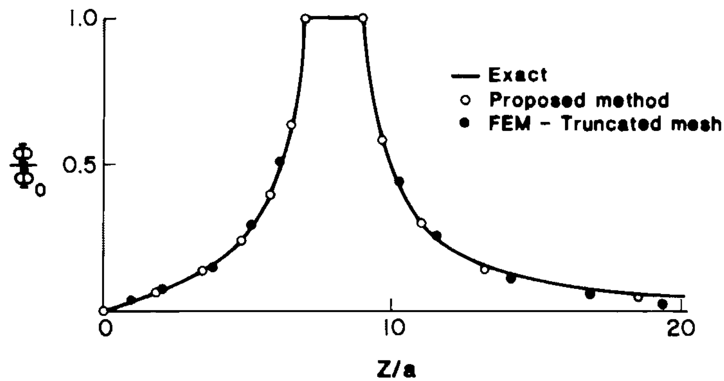

Figure 5: Normalized potential distribution along the z-axis for the system in Fig. 2, for $b/a = 8$

Table 1
Comparison of the results obtained in the transformed and original domains for sphere-to-plane configuration

	Original domain		Transformed domain	
Item	$b/a = 2$	$b/a = 8$	$b/a = 2$	$b/a = 8$
Total number of elements	33	36	15	15
Total number of unknowns	60	65	30	30
Artificial boundary	16a × 16a	16a × 22a	–	–
CPU time on the Amdahl 5850 system	1.77 sec	2.07 sec	0.61 sec	0.61 sec
Error in capacitance	2.66%	4.44%	0.22%	−0.27%

For two extreme values of the ratio b/a, $b/a = 2$ and $b/a = 8$, FEM was also applied in the original domain by considering the potential equal to zero on the boundaries of the truncated region. For the case corresponding to the ratio $b/a = 8$, the potential distributions obtained by the two methods is given in Fig. 5. A comparison between the proposed method and the truncated mesh technique in terms of computational effort is summarized in Table 1.

3.2. Capacitance of a torus in free space

In order to obtain accurate results with a reduced amount of computation, application of the proposed method does not require the transformed domain to have such a simple geometric shape as that in Example 3.1. To illustrate this, consider the application of the standard inversion transformation for calculating the capacitance of a torus. The azimuthal section of a conducting torus of circular cross section is shown in Fig. 6. As in Example 3.1, the capacitance of this torus can be determined from the minimum value of the functional

$$F = \frac{\varepsilon_0}{2} \int_D \rho (\nabla \Phi)^2 \, \mathrm{d}z \, \mathrm{d}\rho \tag{22}$$

with the constraints

$$\Phi = \begin{cases} \Phi_0 & \text{for } z^2 + (\rho - b)^2 = a^2 \\ 0 & \text{at infinity} \end{cases} \tag{23}$$

The inversion with respect to the circle $z^2 + (\rho - b)^2 = a^2$ is given by the trans-

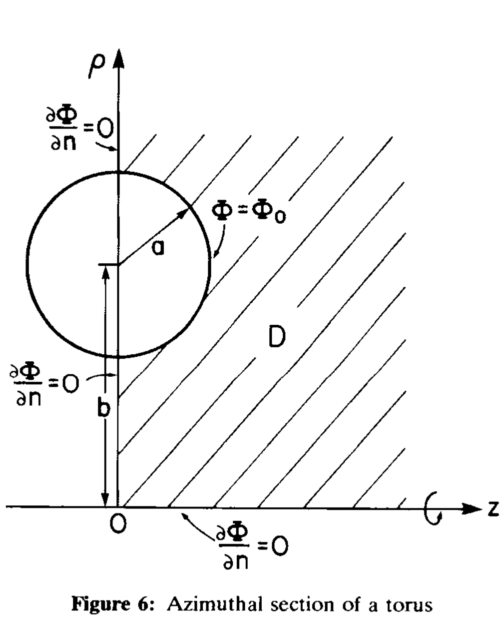

Figure 6: Azimuthal section of a torus

formation function $f(w) = a/w + ib$, which yields

$$z = \frac{au}{u^2 + v^2} \tag{24}$$

$$\rho = -\frac{av}{u^2 + v^2} + b \tag{25}$$

The transformed domain D' is shown in Fig. 7 and eqs. (22) and (23) become, respectively,

$$F = \frac{\varepsilon_0}{2} \int_{D'} \rho'(\nabla'\Phi')^2 \, \mathrm{d}u \, \mathrm{d}v \tag{26}$$

and

$$\Phi' = \begin{cases} \Phi_0 & \text{for } u^2 + v^2 = 1 \\ 0 & u = v = 0 \end{cases} \tag{27}$$

The function ρ' in eq. (26) can be written in polar coordinates as (see Fig. 7)

$$\rho'(r, \theta) = -\frac{a \sin \theta}{r} + b \tag{28}$$

For a ratio of $b/a = 8$, the mesh used in the transformed domain is presented in Fig. 7 and consists of 30 quadratic elements. The exact value of the capacitance

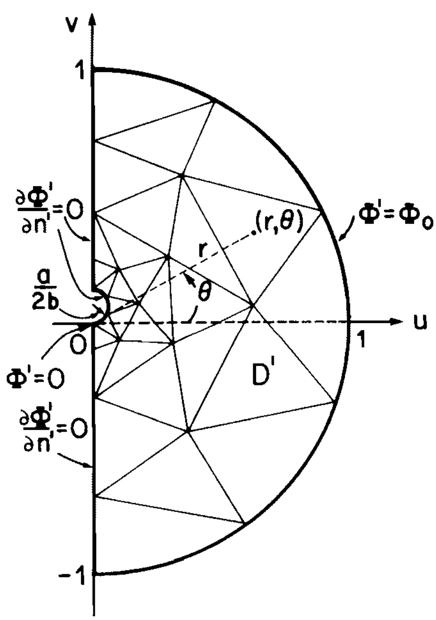

Figure 7: Finite element mesh in the transformed domain for Example 3.2

normalized with respect to $4\pi\varepsilon_0 a$ was determined [12] as being 6.1007 ± 0.00092. The result obtained by the present method is 6.148.

3.3. Conducting sphere in an inhomogeneous dielectric

As an example of a field problem involving inhomogeneities, consider a conducting sphere of radius a in an infinitely extended inhomogeneous dielectric. The electric potential of the sphere is Φ_0 with respect to the zero potential at infinity. The variation of the permittivity ε of the dielectric is chosen to be

$$\varepsilon = \varepsilon_0\left(\frac{10a}{R} + 1\right) \tag{29}$$

where R denotes the radial distance from the center of the sphere.

The original domain D is now mapped onto a bounded domain D' by using the inversion transformation function $f(w) = a/w$, as illustrated in Fig. 8, and the transformed functional in eq. (9) is now

$$F = \frac{-\varepsilon_0 a}{2} \int_{D'} \frac{v}{u^2 + v^2} (10\sqrt{u^2 + v^2} + 1)(\nabla'\Phi')^2 \, du \, dv \tag{30}$$

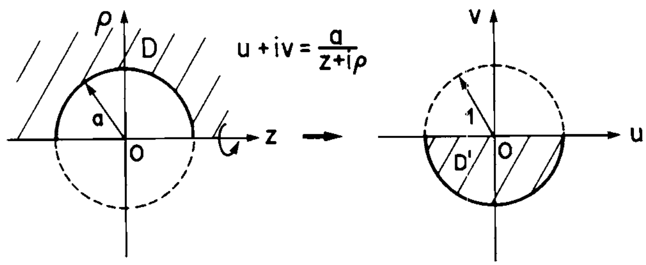

Figure 8: Mapping by inversion for exterior-field problems relative to a sphere

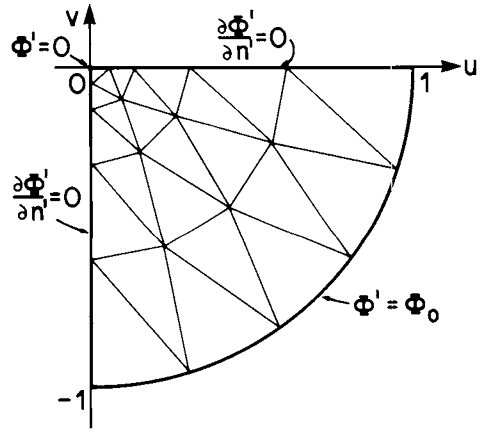

Figure 9: Finite element mesh in the transformed domain for Examples 3.3 and 3.4

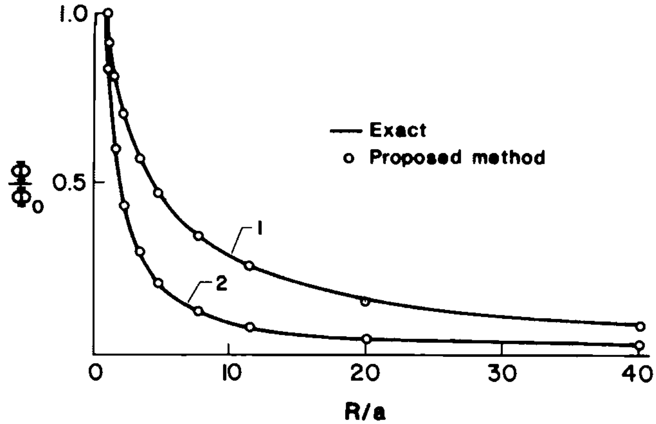

Figure 10: Normalized potential distribution in the radial direction: (1) Conducting sphere in inhomogeneous dielectric medium (Example 3.3); (2) Conducting sphere with external source distribution (Example 3.4)

Taking into account the symmetry with respect to the v-axis, the problem was solved for the quadrant shown in Fig. 9, with a mesh of 25 quadratic elements. The potential distribution obtained is given in Fig. 10 and the calculated normalized electrostatic capacitance, $C = F_{\min}/(\varepsilon_0 a \Phi_0^2)$ is 0.68% above its exact value of 10/ln 11.

3.4. Charged sphere with external source distribution

To test the proposed method for the solution of the nonhomogeneous equation (1), consider now a conducting sphere of radius a in an infinitely extended homogeneous dielectric with a source distribution outside the sphere given by (see eq. (1))

$$g = \frac{1}{R^4} \tag{31}$$

where R is the distance from the center of the sphere.

The same transformation and mesh used in Example 3.3 were considered for this problem. The normalized potential distribution obtained is shown in Fig. 10. Within a radial distance of 11 times the radius of the sphere, the maximum percentage error in nodal potentials is 1.04%.

DISCUSSION

From the examples considered, one can see that the proposed method is well suited to solving scalar field problems in unbounded regions. When mapping an unbounded axisymmetric region onto a bounded domain, a factor which is singular at the point corresponding to infinity in the original domain will appear in the integrand of the transformed functional (such as $1/r$ in eq. (28)). In order to evaluate the transformed functional in eq. (9), the trial functions used in the FEM must be chosen properly. Lagrangian polynomial shape functions of order n are adequate even for problems in which the radial distance function ρ' in eq. (9) has a singularity of the order $0(1/r^{2n-1})$. In the case of inversion mapping, ρ' has a singularity of the order $0(1/r)$ and, therefore, even linear elements can be used.

The numerical evaluation of the integral in eq. (9) can be performed by applying standard quadrature formulas [13] and this constitutes an advantage of the method presented. As illustrated in Example 3.1, the solution for the whole range of geometric parameters can be obtained by using the same mesh in the transformed domain, shown in Fig. 3. In such cases, the analysis in the original domain would have required a different mesh for each set of parameters characterizing the system geometry.

In the examples considered, much more accurate results were obtained for approximately half the number of unknowns in the transformed domains, as compared to the truncated mesh technique in the original domains.

4. CONCLUSIONS

A very simple technique of using conformal mapping in the finite-element solution of unbounded region axisymmetric field problems has been presented. By transforming directly the functional incorporating the boundary conditions of the original problem, there is no approximation made regarding the boundary conditions and the behaviour of the field quantities towards infinity. This greatly enhances the accuracy of the numerical results.

Since the transformed functional is similar to the original one and special quadrature techniques are not required, any standard finite-element computer program can be used for the implementation of this method.

The usage of the presented procedure is straightforward and simple even for problems with material inhomogeneities, as illustrated in Example 3.3, or in anisotropic media. As shown in the comparative Table 1 for a characteristic tested example, the proposed method is efficient, yielding highly accurate results with a substantially reduced amount of computation.

The general procedure presented in this paper is not restricted to the scalar axisymmetric fields considered for illustration. It can also be applied to the analysis of other scalar and even vector axisymmetric field problems.

ACKNOWLEDGEMENT

Financial support for this work from the Natural Sciences and Engineering Research Council of Canada is gratefully acknowledged.

REFERENCES

[1] M.A. Jaswon and G.T. Symm, Integral Equation Methods in Potential Theory and Elastostatics (Academic Press, London, 1977).

[2] P. Silvester and M.S. Hsieh, Finite-element solution of 2-dimensional exterior-field problems, Proc. IEE 118 (1971) 1743–1747.

[3] B.H. McDonald and A. Wexler, Finite-element solution of unbounded field problems, IEEE Trans. on Microwave Theory and Techniques MTT-20 (1972) 841–847.
[4] P. Bettess, Infinite elements, Int. J. Num. meth. Engng. 11 (1977) 53–64.
[5] F. Medina, An axisymmetric infinite element, Int. J. Num. meth. Engng. 17 (1981) 1177–1185.
[6] O.C. Zienkiewicz, C. Emson and P. Bettess, A novel boundary infinite element, Int. J. Num. meth. Engng. 19 (1983) 393–404.
[7] Y. Kagawa, T. Yamabuchi and S. Kitagami, The infinite boundary element method and its application to a combined finite boundary element technique for unbounded field problems, COMPEL 2 (1983) 179–193.
[8] S. Pissanetzky, A simple infinite element, COMPEL 3 (1984) 107–114.
[9] B. Nath and J. Jamshidi, The w-plane finite element method for the solution of scalar field problems in two dimensions, Int. J. Num. meth. Engng. 15 (1980) 361–379.
[10] A.J. Davies, The Finite Element Method (Clarendon Press, Oxford, 1980).
[11] P.M. Morse and H. Feshbach, Methods of Theoretical Physics (McGraw-Hill, New York, 1953).
[12] O. Aboul-Atta, S. Bilgen, I.R. Ciric, B.W. Klimpke, A. Wexler and Y.B. Yildir, Ontario Hydro—GPU HVDC Interconnection ground electrode study, TR 82-1, University of Manitoba (1982).
[13] G.R. Cowper, Gaussian quadrature formulas for triangles, Int. J. Num. meth. Engng. 7 (1973) 405–408.